

Magnetohydrodynamic Oscillatory Viscoelastic Flow with Radiation and Constant Suction over a Vertical Flat Plate in a Porous Medium

¹K. K. Asogwa, ²A. A. Ibe and ³U. M. Udo

^{1,3}Department of Mathematics, Nigeria Maritime University, Okerenkoko, Delta State

²Department of Physics, Nigeria Maritime University, Okerenkoko, Delta State

Abstract: This research work examined Magnetohydrodynamics (MHD) flow over an infinite plate in a porous medium with constant suction, oscillatory viscoelastic and radiation effects. Effects of Grashof numbers, viscoelastic parameter, radiation parameter, Prandtl and Schmidt numbers are discussed. The results found for concentration, temperature and velocity are depicted graphically. The velocity flow field increases with increasing values of thermal Grashof number, mass Grashof number and magnetic field. Hence, the velocity flow field reduces with increasing values of Schmidt number, Prandtl number, reactive term, radiation parameter and porous parameter.

Date of Submission: 18-11-2019

Date of Acceptance: 04-12-2019

I. Introduction

The investigation of mass and heat transfer in fluids has been considered extensively due to their occurrences in several industrial applications by extension in chemical reactions, nuclear reactors, electronic chips and semiconductors, space science and processes involving high temperatures. MHD is of great interest in industrial applications. It is characterized by the observation of the magnetic field which improves fluid viscosity and hence rises the flow resistance. Many works considered the effect of magnetic field on flow structures in various dimensions. (Sahoo, 2013) examined heat and mass transfer effect on MHD flow of a viscoelastic fluid through a porous medium bounded by an oscillating porous plate in slip flow regime, he noticed that the inclusion of Prandtl number decreases the speed of the flow field, where as the presence of magnetic field increases it. (Dulal and Sukanta, 2018) analysed magnetohydrodynamic convective-radiative oscillatory flow of a chemically reactive micro polar fluid in a penetrable medium, they concluded among other observations that velocity profiles increases with increase in time but it drops by increasing the values of the viscosity ratio parameter. (Mohammad Al Zubi, 2018) studied MHD heat and mass transfer of a fluctuation flow over a vertical permeable plate in a medium with chemical reaction, It was found that, augmenting the permeability and chemical reaction parameters will lead to an increase in the fluid momentum. The velocity distribution increases as the magnetic field parameter declines and the concentration decreases as the Schmidt number increases. (Pradip and Abhay, 2016) investigated heat and mass transfer in a viscoelastic fluid through a rotating penetrable channel with hall effect. (Balvinder et al, 2014) discussed hall current effect on Walter's liquid model-B MHD fluctuation convective channel flow through a medium with radiation. (Kandasamy and Khamis, 2006) presented the results of chemical reaction, heat and mass transfer on boundary layer flow over a penetrable wedge with radiation in the influence of suction/injection. (Chamkha, 2003) described MHD fluid flow of invariant stretched perpendicular permeable exterior in the presence of heat generation/absorption and a reactive parameter. (Khadrawi and Al-Odat, 2005) analysed transient MHD free convection flow over a permeable erect moving plate embedded in penetrable medium with uniform suction. (Attia, 2010) studied time dependent MHD Couette flow of a viscoelastic fluid flow with heat transfer.

(Rajgopala et al, 2006) investigated oscillatory movement of an electrically conducting viscous as well as elastic properties fluid over a stretching sheet in saturated porous medium with suction/blowing. (Reddy et al, 2013) studied MHD heat and mass transfer flow of a viscoelastic fluid past an impulsively started infinite perpendicular plate with chemical reaction, (Kishore et al, 2013) described the effects of radiation and chemical reaction on time dependent MHD free convection flow of viscous fluid past an exponentially accelerated perpendicular plate, (Pal and Mandal, 2017) studied thermal energy radiation and MHD effect on partition layer flow of micropolar nanofluid past a stretching sheet with non-uniform heat source/sink, (Sahoo et al, 2003) studied magnetohydrodynamic unsteady free convection flow past an infinite perpendicular plate with no variable suction and heat sink.

The objective of this research work is to study MHD oscillatory viscoelastic flow of a viscous incompressible fluid past a vertical porous plate with radiation and constant suction unlike the above literature this work contains constant suction in porous media.

This work seeks to address the behavior of MHD oscillatory viscoelastic fluid flow with constant suction.

The dimensionless governing equations are solved using analytical method.

Problem Formulation

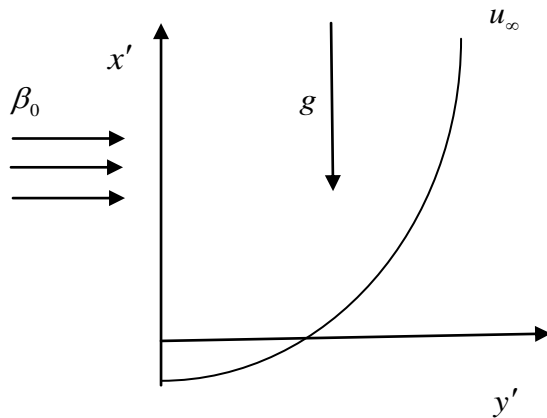


Figure 1. Physical configuration

The dependent 2D flow of an incompressible, viscous, electrically conducting fluid flow past an infinite vertical plate located at the plane $y = 0$ is examined. The x' -axis is chosen along the plate in the upward direction and y' -axis is taken perpendicular to the plate put through to a uniform magnetic field (see Figure 1). The transversely applied magnetic field is assumed to be very small and negligible. Time-dependent wall suction is assumed to occur at the permeable surface. The viscous dissipations is neglected in this research work and the free stream velocity follows the exponentially increasing small perturbation law. In addition, it is assumed that the temperature, concentration at the wall as well as the velocity is exponentially varying with time.

The governing equations of the system for the fluid flow are the momentum, mass concentration and energy respectively (Equations 1, 2 and 3).

$$\frac{\partial u'}{\partial t'} - v_0 \frac{\partial u'}{\partial y'} = \nu \frac{\partial^2 u'}{\partial y'^2} - \sigma \frac{\beta_0^2}{\rho} u' + g\beta(T' - T_\infty) + g\beta^*(C' - C_\infty) - \frac{\sigma B_0^2 u'}{\rho} - \nu \frac{u'}{k^*} - k_0 \frac{\partial^3 u'}{\partial t \partial y^3} \tag{1}$$

$$\frac{\partial C'}{\partial t'} - v_0 \frac{\partial C'}{\partial y'} = D \frac{\partial^2 C'}{\partial y'^2} - k^* C' \tag{2}$$

$$\frac{\partial T'}{\partial t'} - v_0 \frac{\partial T'}{\partial y'} = \frac{k}{\rho C_p} \frac{\partial^2 T'}{\partial y'^2} - \frac{1}{\rho C_p} \frac{\partial q_r}{\partial y'} + Q_0(T_0 - T') \tag{3}$$

The initial and boundary conditions are:

$$\left. \begin{aligned} t < 0 : u' = 0, C' = 0, T' = 0 \quad \text{for all } y \\ t \geq 0 : u' = u_0 e^{i\zeta' t'}, C' = C_\infty + (C_0 - C_\infty) e^{i\zeta' t'}, \\ T' = T_\infty + (T_0 - T_\infty) e^{i\zeta' t'} \end{aligned} \right\} \tag{4}$$

Assuming the radiative thermal flux from the Rosseland approximation (Boussinesq 1897), is

$$\frac{\partial q_r}{\partial y'} = -\frac{4\sigma}{3k^*} (T_\infty'^4 - T'^4) \tag{5}$$

σ is the Stefan Boltzmann, k^* is the mean absorption effect for thermal radiation constant. We assume that the temperature differences within the flow are sufficiently small such that T'^4 can be expanded in a Taylor series about T'_∞ and neglecting higher order terms give

$$T'^4 = 4T'T_\infty'^3 - 3T_\infty'^4 \tag{6}$$

Hence (5) becomes

$$\frac{\partial q_r}{\partial y'} = \frac{16\sigma T_\infty'^3 (T' - T'_\infty)}{3k^*} \tag{7}$$

Substituting in (7) into (3) gives

$$\frac{\partial T'}{\partial t'} - \nu_0 \frac{\partial T'}{\partial y'^2} = \frac{k}{\rho C_p} \frac{\partial^2 T'}{\partial y'^2} - \frac{16\sigma T_\infty'^3 (T' - T'_\infty)}{3k^* \rho C_p} + Q_0 (T_0 - T') \tag{8}$$

Introducing the following dimensionless quantities

$$\left. \begin{aligned} u &= \frac{u'}{u_0}, t = \frac{\nu_0^2 t'}{4\nu}, \zeta = \frac{4\nu \zeta'}{\nu_0^2}, y = \frac{y' \nu_0}{\nu}, \text{Pr} = \frac{\nu \rho C_p}{k}, S = \frac{4Q_0 \nu}{\nu_0^2}, Gr = \frac{g \beta \nu (T_0 - T_\infty)}{\nu_0^2 u_0}, \\ Gc &= \frac{g \beta^* \nu (C_0 - C_\infty)}{\nu_0^2 u_0}, Sc = \frac{\nu}{D}, R = \frac{64\sigma T_0^3 \nu^2}{\nu_0^2 k}, k_o = \frac{k_0^* \nu_0^2}{\nu}, M = \frac{4\sigma B_0^2 \nu}{\nu_0^2 \rho}, \\ a &= \frac{4\nu}{\nu_0^2 k^*}, \theta = \frac{T' - T_\infty}{T_0 - T_\infty}, C = \frac{C' - C_\infty}{C_0 - C_\infty} \end{aligned} \right\} \tag{9}$$

The equations 1, 2, 3 and 8 reduce to

$$\frac{1}{4} \frac{\partial u}{\partial t} - \frac{\partial u}{\partial y} = Gr\theta + GcC + \frac{\partial^2 u}{\partial y^2} - \frac{(M + a)}{4} u - \frac{k_o}{4} \frac{\partial^3 u}{\partial t \partial y^3} \tag{10}$$

$$\frac{1}{4} \frac{\partial C}{\partial t} - \frac{\partial C}{\partial y} = \frac{1}{Sc} \frac{\partial^2 C}{\partial y^2} - \frac{k}{4} C \tag{11}$$

$$\frac{1}{4} \frac{\partial \theta}{\partial t} - \frac{\partial \theta}{\partial y} = \frac{1}{\text{Pr}} \frac{\partial^2 \theta}{\partial y^2} - \frac{1}{4} (F + s) \theta \tag{12}$$

The initial and boundary conditions imposed are

$$\left. \begin{aligned} t < 0 : u = 0, C = 0, \theta = 0, & \quad \text{for all } y \\ t > 0 : u = e^{i\zeta t}, C = e^{i\zeta t}, \theta = e^{i\zeta t}, & \quad y = 0 \\ u \rightarrow 0, C \rightarrow 0, \theta \rightarrow 0, & \quad y \rightarrow \infty \end{aligned} \right\} \tag{13}$$

Where Gr is thermal grashofnumber, Gc is the mass grashof number, Sc is the Schmidt number, Pr is the Prandtl number, and $F = \frac{R}{\text{Pr}}$, R and k are the radiation and reactive parameters respectively. k_0 is viscoelastic parameter, a is the porous parameter and S is the heat sink/source parameter.

II. Methodology

Assumed solutions to (10), (11) and (12) in the form

$$u(y, t) = u_1(y) e^{i\zeta t} \tag{14}$$

$$C(y, t) = C_1(y) e^{i\zeta t} \tag{15}$$

$$\theta(y, t) = \theta_1(y) e^{i\zeta t} \tag{16}$$

where $u_1(y)$, $C_1(y)$ and $\theta_1(y)$ are to be determined. Substituting (14), (15) and (16) into (10) to (12) with the boundary conditions (13) the following equations were obtained.

$$C_1'' + ScC_1' - \frac{Sc}{4}(k + i\zeta)C_1 = 0 \tag{17}$$

$$\theta_1'' + Pr\theta_1' - \frac{Pr}{4}(F + s + i\zeta)\theta_1 = 0 \tag{18}$$

$$\left(1 - i\zeta \frac{k_0}{4}\right)u_1'' + u_1' - \frac{1}{4}(M + a + i\zeta)u_1 = -Gr\theta_1 - GcC_1 \tag{19}$$

The boundary conditions are:

$$\left. \begin{aligned} u_1 = 1, C_1 = 1, \theta_1 = 1 & \quad \text{at } y = 0 \\ u_1 \rightarrow 0, C_1 \rightarrow 0, \theta_1 \rightarrow 0, y \rightarrow \infty \end{aligned} \right\} \tag{20}$$

Solving equations (17) to (19) subject to the boundary conditions (20), we obtain

$$\theta_1(y) = e^{-\alpha y} \tag{21}$$

$$C_1(y) = e^{-\gamma y} \tag{22}$$

$$u_1(y) = e^{-by} + \frac{Gr}{\eta_1}(e^{-by} - e^{-\alpha y}) + \frac{Gc}{\eta_2}(e^{-by} - e^{-\gamma y}) \tag{23}$$

where

$$\alpha = \frac{1}{2} \left\{ Pr + \sqrt{Pr^2 + Pr(F + s + i\zeta)} \right\}, \quad \gamma = \frac{1}{2} \left\{ Sc + \sqrt{Sc^2 + Sc(k + i\zeta)} \right\},$$

$$b = \left(1 + \sqrt{\left[1 + \left(1 - \frac{i\zeta k_0}{4} \right) (M + a + i\zeta) \right]} \right) / 2 \left(1 - \frac{i\zeta k_0}{4} \right)$$

$$\eta_1 = \left(1 - i \frac{\zeta k_0}{4} \right) \alpha^2 - \alpha - \frac{1}{4}(M + a + i\zeta), \quad \eta_2 = \left(1 - i \frac{\zeta k_0}{4} \right) \gamma^2 - \gamma - \frac{1}{4}(M + a + i\zeta)$$

Substituting (17) to (20) into (10) to (12) and separating into real and imaginary parts we obtain

$$\theta(y, t) = e^{-\frac{y}{2} \left(Pr + f_0 \cos \frac{\phi}{2} \right)} \left\{ \cos \left(\zeta t - \frac{y}{2} f_0 \sin \frac{\phi}{2} \right) + i \sin \left(\zeta t - \frac{y}{2} f_0 \sin \frac{\phi}{2} \right) \right\} \tag{24}$$

$$f_0 = \left\{ \left(Pr^2 + Pr(F + s) \right)^2 + \zeta^2 Pr^2 \right\}^{\frac{1}{4}}, \quad \phi = \tan^{-1} \left(\frac{\zeta}{Pr + F + s} \right)$$

Where

$$C(y, t) = e^{-\frac{y}{2} \left(Sc + f_1 \cos \frac{\psi}{2} \right)} \cos \left(\zeta t - \frac{y}{2} f_1 \sin \frac{\psi}{2} \right) + i e^{-\frac{y}{2} \left(Sc + f_1 \cos \frac{\psi}{2} \right)} \sin \left(\zeta t - \frac{y}{2} f_1 \sin \frac{\psi}{2} \right) \tag{25}$$

$$f_1 = \left\{ \left(Sc^2 + kSc \right)^2 + \zeta^2 Sc^2 \right\}^{\frac{1}{4}}, \quad \psi = \tan^{-1} \left(\frac{\zeta}{Sc + k} \right)$$

where

Similarly,

$$u(y, t) = \delta_r(y) + i\delta_i(y) \tag{26}$$

where

$$\delta_r(y) = e^{-b_1 y} \cos(\zeta t - b_2 y) + \frac{Gr}{A_1^2 + A_2^2} \left\{ A_1 \left(e^{-b_1 y} \cos(\zeta t - b_2 y) - e^{-\frac{y}{2}(\text{Pr} + f_0 \cos \frac{\phi}{2})} \cos\left(\zeta t - \frac{y}{2} f_0 \sin \frac{\phi}{2}\right) \right) \right. \\ \left. + A_2 \left(e^{-b_1 y} \sin(\zeta t - b_2 y) - e^{-\frac{y}{2}(\text{Pr} + f_0 \cos \frac{\phi}{2})} \sin\left(\zeta t - \frac{y}{2} f_0 \sin \frac{\phi}{2}\right) \right) \right\} + \frac{Gc}{A_3^2 + A_4^2} \left\{ A_3 \left(e^{-b_1 y} \cos(\zeta t - b_2 y) - e^{-\frac{y}{2}(Sc + f_1 \cos \frac{\psi}{2})} \right. \right. \\ \left. \left. \times \cos\left(\zeta t - \frac{y}{2} f_1 \sin \frac{\psi}{2}\right) \right) + A_4 \left(e^{-b_1 y} \sin(\zeta t - b_2 y) - \sin\left(\zeta t - \frac{y}{2} f_1 \sin \frac{\psi}{2}\right) e^{-\frac{y}{2}(Sc + f_1 \cos \frac{\psi}{2})} \right) \right\}$$

$$\delta_i(y) = e^{-b_1 y} \sin(\zeta t - b_2 y) + \frac{Gr}{A_1^2 + A_2^2} \left\{ A_1 \left(e^{-b_1 y} \sin(\zeta t - b_2 y) - e^{-\frac{y}{2}(\text{Pr} + f_0 \cos \frac{\phi}{2})} \sin\left(\zeta t - \frac{y}{2} f_0 \sin \frac{\phi}{2}\right) \right) \right. \\ \left. - A_2 \left(e^{-b_1 y} \cos(\zeta t - b_2 y) - e^{-\frac{y}{2}(\text{Pr} + f_0 \cos \frac{\phi}{2})} \cos\left(\zeta t - \frac{y}{2} f_0 \sin \frac{\phi}{2}\right) \right) \right\} + \frac{Gc}{A_3^2 + A_4^2} \left\{ A_3 \left(e^{-b_1 y} \sin(\zeta t - b_2 y) - e^{-\frac{y}{2}(Sc + f_1 \cos \frac{\psi}{2})} \right. \right. \\ \left. \left. \times \sin\left(\zeta t - \frac{y}{2} f_1 \sin \frac{\psi}{2}\right) \right) - A_4 \left(e^{-b_1 y} \cos(\zeta t - b_2 y) - \cos\left(\zeta t - \frac{y}{2} f_1 \sin \frac{\psi}{2}\right) e^{-\frac{y}{2}(Sc + f_1 \cos \frac{\psi}{2})} \right) \right\}$$

$$A_1 = \frac{1}{4} \left(\text{Pr}^2 + 2f_0 \text{Pr} \cos \frac{\phi}{2} + f_0^2 \cos \phi + \frac{\zeta k_0 \text{Pr} f_0}{2} \sin \frac{\phi}{2} + \frac{\zeta k_0 f_0^2}{4} \sin \phi \right) - \frac{1}{2} \left(\text{Pr} + f_0 \cos \frac{\phi}{2} \right) - \frac{1}{4} (M + a)$$

$$A_2 = \frac{1}{4} \left(2\text{Pr} f_0 \sin \frac{\phi}{2} + f_0^2 \sin \phi - \frac{\zeta k_0 \text{Pr}^2}{4} - \frac{\zeta k_0 \text{Pr} f_0}{2} \cos \frac{\phi}{2} - \frac{\zeta k_0 f_0^2}{4} \cos \phi \right) - \frac{f_0}{2} \sin \frac{\phi}{2} - \frac{\zeta}{4}$$

$$A_3 = \frac{1}{4} \left(Sc^2 + 2Scf_1 \cos \frac{\psi}{2} + f_1^2 \cos \psi + \frac{\zeta k_0 Scf_1}{2} \sin \frac{\psi}{2} + \frac{\zeta k_0 f_1^2}{4} \sin \psi \right) - \frac{1}{2} \left(Sc + f_1 \cos \frac{\psi}{2} \right) - \frac{1}{4} (M + a)$$

$$A_4 = \frac{1}{4} \left(2Scf_1 \sin \frac{\psi}{2} + f_1^2 \sin \psi - \frac{\zeta k_0 Sc^2}{4} - \frac{\zeta k_0 Scf_1}{2} \cos \frac{\psi}{2} - \frac{\zeta k_0 f_1^2}{4} \cos \psi \right) - \frac{f_1}{2} \sin \frac{\psi}{2} - \frac{\zeta}{4}$$

$$b_1 = \frac{8}{16 + \zeta^2 k_0^2} \left(1 + f_2 \cos \frac{\eta}{2} - \frac{\zeta k_0 f_2}{4} \sin \frac{\eta}{2} \right), b_2 = \frac{8}{16 + \zeta^2 k_0^2} \left(f_2 \sin \frac{\eta}{2} + \frac{\zeta k_0}{4} \left(1 + f_2 \cos \frac{\eta}{2} \right) \right)$$

$$f_2 = \left\{ \left(1 + M + a + \frac{\zeta^2 k_0}{4} \right)^2 + \zeta^2 \left(1 - \frac{k_0}{4} (M + a) \right)^2 \right\}^{\frac{1}{4}}, \quad \eta = \tan^{-1} \left\{ \frac{\zeta \left(1 - \frac{k_0}{4} (M + a) \right)}{1 + M + a + \frac{\zeta^2 k_0}{4}} \right\}$$

Nusselt number

$$-\frac{\partial \theta}{\partial y} \Big|_{y=0} = \frac{1}{2} \left\{ \text{Pr} \cos \zeta t + f_0 \cos \left(\frac{\phi}{2} + \zeta t \right) + i \left(\text{Pr} \sin \zeta t + f_0 \sin \left(\frac{\phi}{2} + \zeta t \right) \right) \right\} \tag{27}$$

Sherwood number

$$-\frac{\partial C}{\partial y}\Big|_{y=0} = \frac{1}{2} \left\{ Sc \cos \zeta t + f_1 \cos \left(\frac{\psi}{2} + \zeta t \right) + i \left(Sc \sin \zeta t + f_1 \sin \left(\frac{\psi}{2} + \zeta t \right) \right) \right\} \tag{28}$$

Skin friction

$$-\frac{\partial u}{\partial y}\Big|_{y=0} = l_r + i l_i \tag{29}$$

where

$$\begin{aligned} l_r &= l_1 \cos \zeta t - l_2 \sin \zeta t, \quad l_i = l_1 \sin \zeta t + l_2 \cos \zeta t \\ l_1 &= b_1 + \frac{Gr}{A_1^2 + A_2^2} \left\{ A_1 \left(b_1 - \frac{1}{2} \left(Pr + f_0 \cos \frac{\phi}{2} \right) \right) + A_2 \left(b_2 - \frac{1}{2} f_0 \sin \frac{\phi}{2} \right) \right\} \\ &+ \frac{Gc}{A_3^2 + A_4^2} \left\{ A_3 \left(b_1 - \frac{1}{2} \left(Sc + f_1 \cos \frac{\psi}{2} \right) \right) + A_4 \left(b_2 - \frac{1}{2} f_1 \sin \frac{\psi}{2} \right) \right\} \\ l_2 &= b_2 + \frac{Gr}{A_1^2 + A_2^2} \left\{ A_1 \left(b_2 - \frac{1}{2} f_0 \sin \frac{\phi}{2} \right) + A_2 \left(\frac{1}{2} f_0 \cos \frac{\phi}{2} - b_1 \right) \right\} \\ &+ \frac{Gc}{A_3^2 + A_4^2} \left\{ A_3 \left(b_2 - \frac{1}{2} f_1 \sin \frac{\psi}{2} \right) + A_4 \left(\frac{1}{2} f_1 \cos \frac{\psi}{2} - b_1 \right) \right\} \end{aligned}$$

III. Results and Discussion

The differential equations (17) to (19) with boundary condition (20) is solved analytically using perturbation technique and the computation was done using the MATLAB R2017a software package. The solutions are obtained for the unsteady velocity field (26), temperature field (24) and concentration field (25) respectively. The effect of each of the parameters present in the system are studied. The results are presented in graphical form. It is supposed that the temperature disparity is small enough so that the density discrepancies of the fluid in the system will be negligible. (Mohammad, 2018)

Figure 2. depicts the discrepancy of the temperature profile for different values of the Prandtl number with the field flow. It is observed from this figure that the temperature profile decreases as the values of Prandtl number increases. This is due to the fact that little values of Prandtl number increases the thermal conductivity of the fluid flow and consequently heat is dissipated from the heated surface more quickly than for higher values of Prandtl number. The presence of heat source increases the temperature of the fluid flow. (Mebarek-Oudina and Makinde 2018)

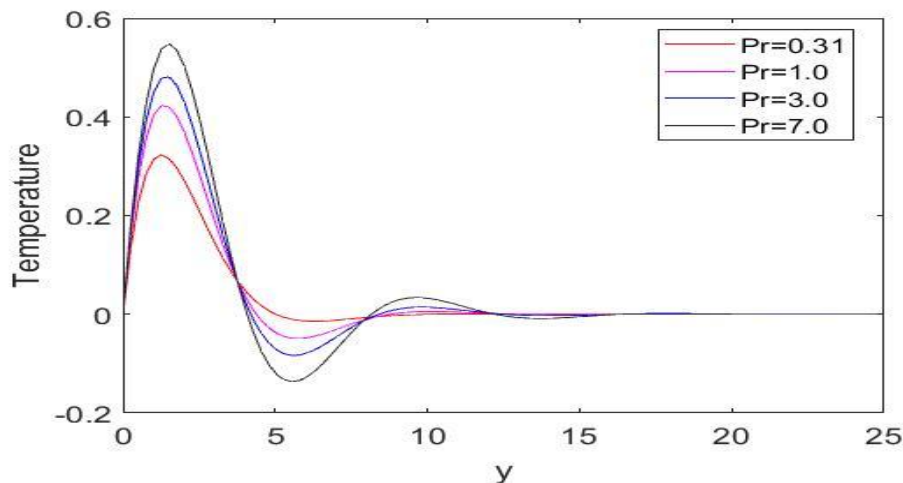


Figure 2: Temperature variation with Prandtl numbers at $\zeta t = \frac{\pi}{2}$

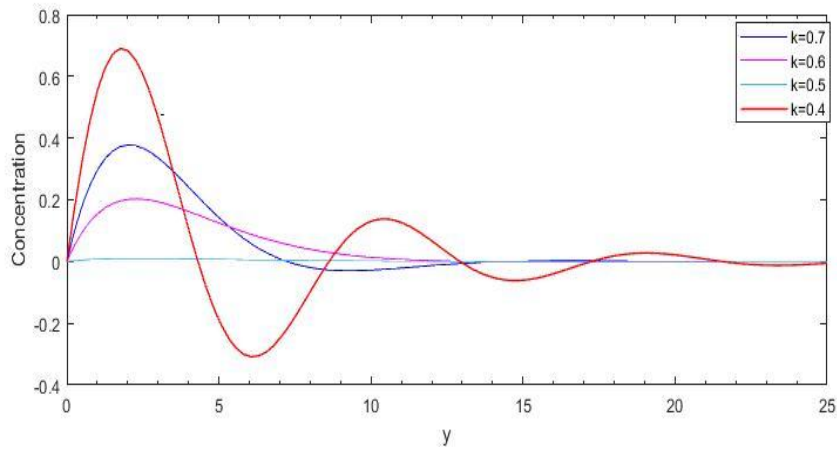


Figure 3: Concentration variation with k at $\zeta t = \frac{\pi}{2}$

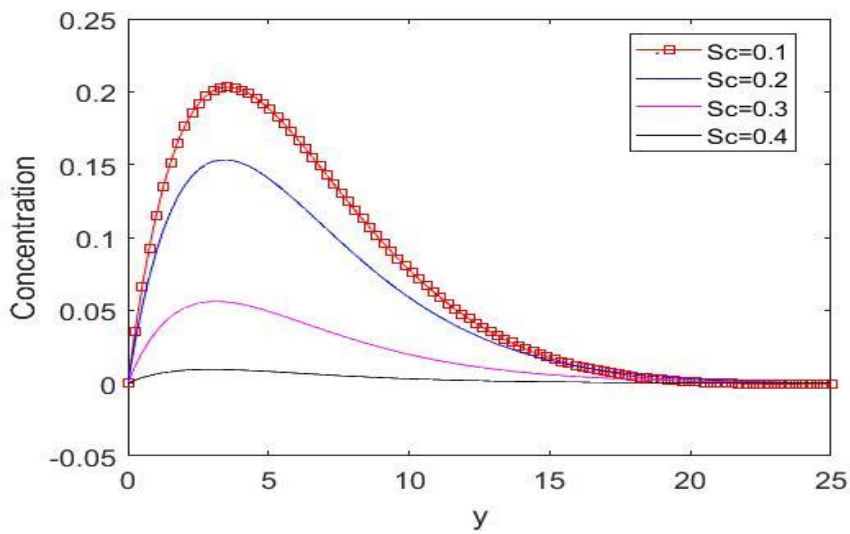


Figure 4: Concentration variation with Schmidt number at $\zeta t = \frac{\pi}{2}$

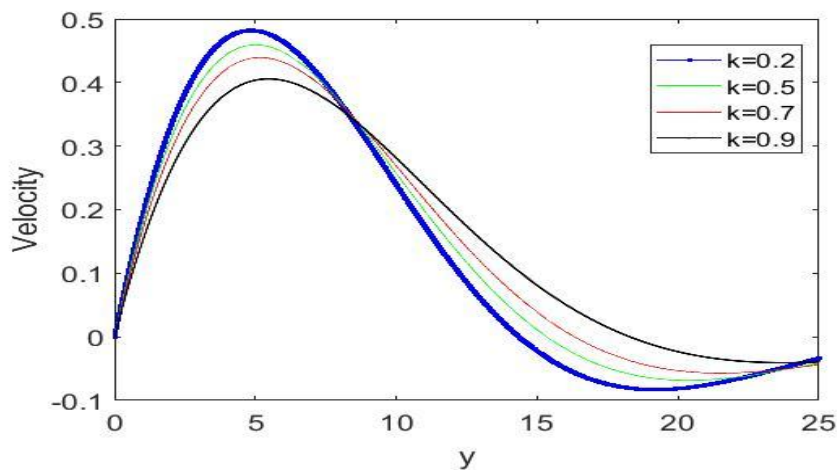


Figure 5: Velocity variation with k at $\zeta t = \frac{\pi}{2}$

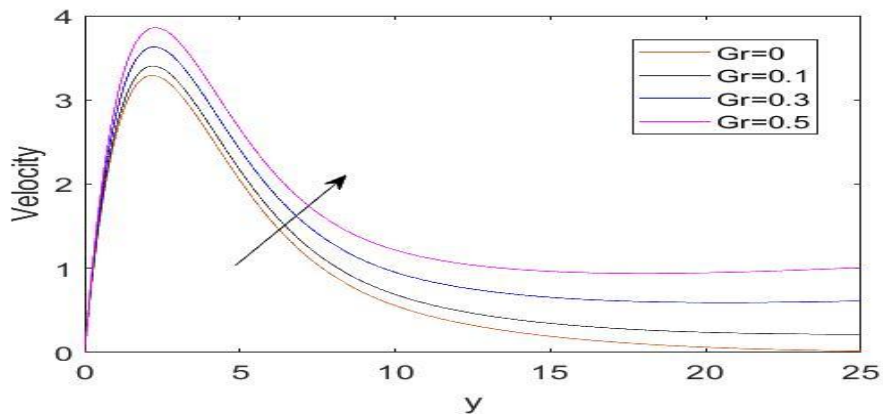


Figure 6: Velocity variation with Gr at $\zeta t = \frac{\pi}{2}$

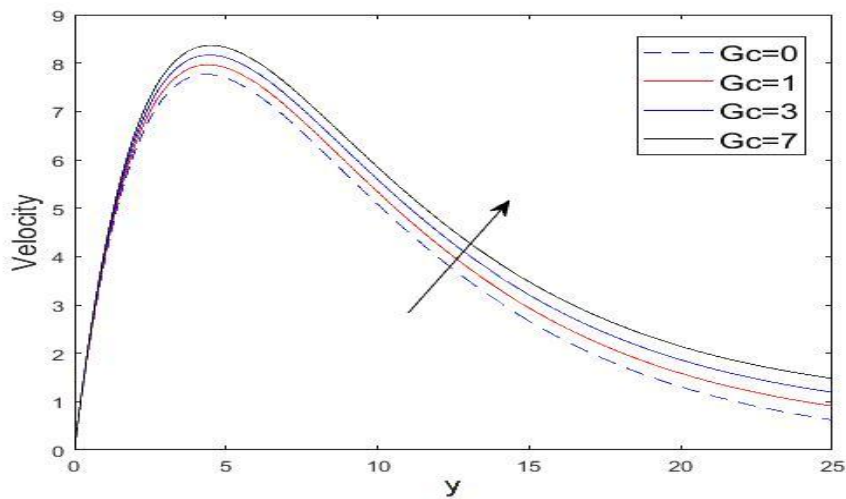


Figure 7: Velocity variation with Gc at $\zeta t = \frac{\pi}{2}$

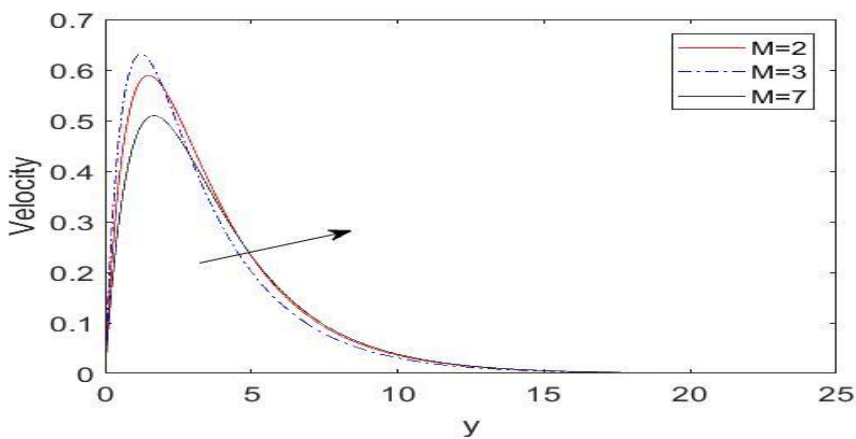


Figure 8: Velocity variation with magnetic number at $\zeta t = \frac{\pi}{2}$

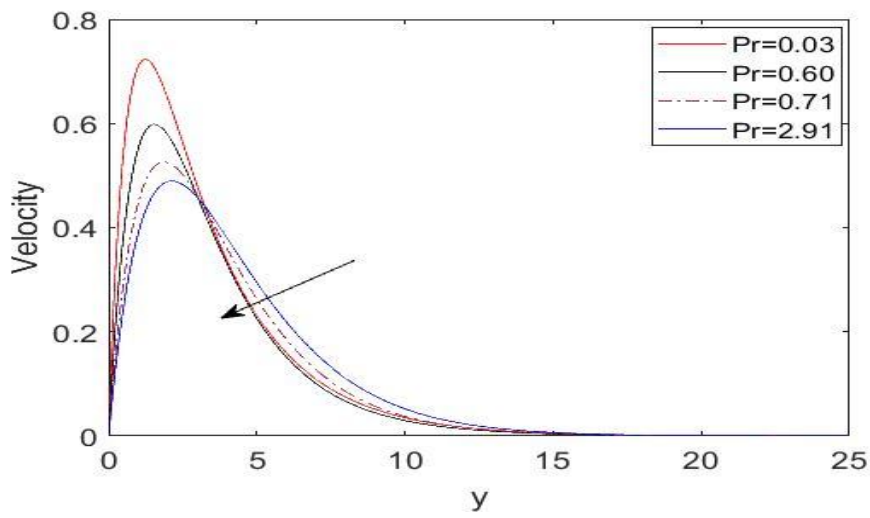


Figure 9: Velocity variation with Prandtl number at $\zeta t = \frac{\pi}{2}$

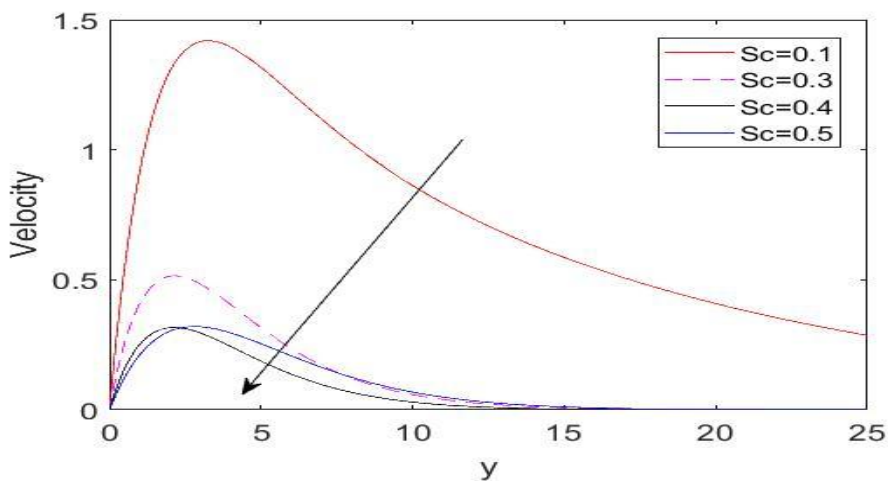


Figure 10: Velocity variation with Schmidt number at $\zeta t = \frac{\pi}{2}$

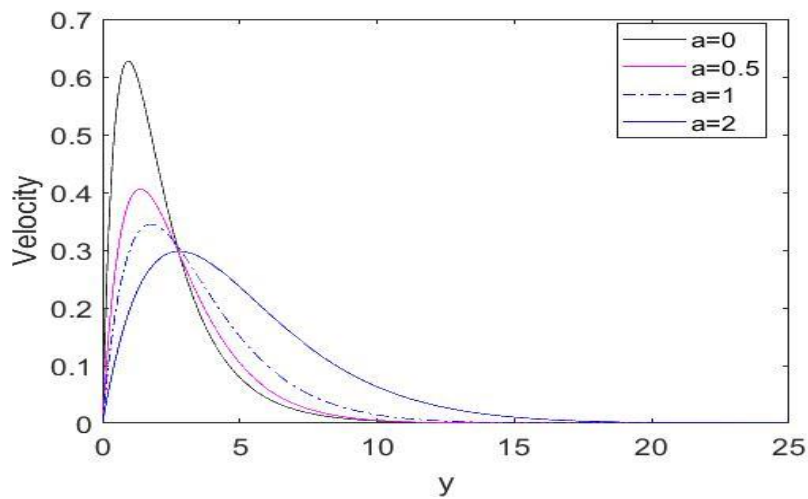


Figure 11: Velocity variation with porosity number at $\zeta t = \frac{\pi}{2}$

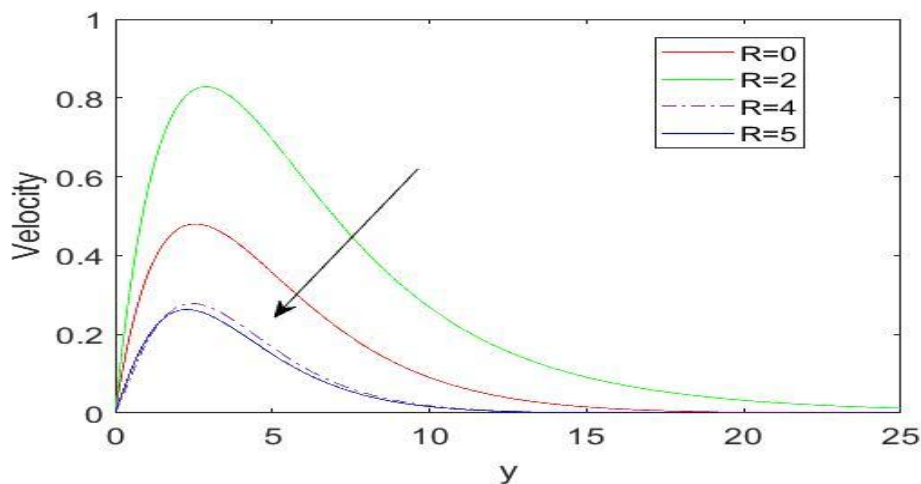


Figure 12: Velocity variation with radiation parameter at $\zeta t = \frac{\pi}{2}$

Figure 3 depicts the disparity of the concentration profile for various values of the reactive parameter. It is observed from this figure that the concentration profile decreases by increasing the values of reactive parameter. It is also noticed that a destructive reaction greater than zero reduces the concentration profile. (Sahoo *et al.*, 2003)

Figure 4 shows the discrepancy of the concentration profile for various values of the Schmidt number. It is seen from this figure that the concentration profile decreases by increasing the values of Schmidt number. This validates that the heavier diffusing species have a greater retarding effect on the concentration profile of the flow field (Sahoo, 2013).

Figure 5 depicts the differential of the velocity profile for various values of the reactive parameter. It is found from this figure that the velocity profile decreases by increasing the values of reactive parameter. It is evident that the increase in the chemical reaction significantly alters the concentration boundary layer thickness but does not alter the momentum boundary layers

Figure 6 shows the disparity of the velocity profile for various values of the thermal Grashof number. It is found from this figure that the velocity profile increases by increasing the values of Gr. The Grashof number signifies the relative effect of the thermal buoyancy force to the viscous hydrodynamic force in the boundary layer. It is seen that there is a rise in the velocity due to the enhancement of thermal buoyancy force. (Sahoo, 2013).

Figure 7 shows the variation of the velocity profile for various values of the mass Grashof number. It is seen from this figure that the velocity profile increases by increasing values of Gc. An increase in Grashof number Gc for mass transfer increases the skin friction and declines the rate of heat transfer. Gc is the ratio of the species buoyancy force to the viscous hydrodynamic force.

Figure 8 shows the disparity of the velocity profile for different values of Magnetic field (M). It is found from this figure that the velocity profile increases by increasing values of M. This is because when M increases, it gives rise to a force called the Lorentz force which acts against the flow if applied in the normal direction (Dulal and Sukanta, 2018).

Figure 9 depicts the disparity of the velocity profile for various values of Pr. It is found from this figure that the velocity profile decreases by increasing values of Pr. If Pr increases, the kinematic viscosity of the fluid dominates the thermal diffusivity of the fluid flow which leads to decreasing the velocity of the flow field. The application of transverse magnetic field sets up the Lorentz force, which enhances the fluid velocity.

Figure 10 shows the variation of the velocity profile for different values of Sc. It is found from this figure that the velocity profile decreases by increasing values of Sc. Increase in Schmidt number (Sc) causes the skin friction to decrease and the rate of heat transfer to increase. Physically it relates the relative thickness of the hydrodynamic layer and mass diffusivity. A larger value of Sc means presence of a heavier fluid hence decrease in skin friction, and increase in the rate of heat transfer (Chamkha, 2003).

Figure 11 shows the variation of the velocity profile for different values of α . It is found from this figure that the velocity profile decreases by increasing values of α .

Figure 12 depicts the differential of the velocity profile for various values of R. It is found from this figure that the velocity profile decreases by increasing values of R. The radiation parameter R defines the

relative contribution of conduction heat transfer to thermal radiation transfer. It is obvious that an increase in the radiative parameter results in decreasing velocity and temperature within the boundary layer.

IV. Conclusions

In this research article, an MHD oscillatory viscoelastic flow with radiation and constant suction over a vertical flat plate in a porous medium has been investigated. Some of the significant points of the present work are listed as below:

- (1) The effect of mass and heat transfer is not significantly affected by the viscoelastic parameter in the flow region.
- (2) Velocity is increasing with increasing Gr, Gc and M . Also, velocity reducing with increasing Sc, Pr, k, R and a . The fluid temperature and concentration is reduced by increase in the values of Pr, k and Sc respectively.
- (3) Increasing values of Magnetic parameter, Prandtl number, Grashof number for Mass transfer and heat source parameter accelerate the flow past a heated plate but a reverse behavior is experienced during the flow past a cooled plate (Dulal and Sukanta, 2018).

References

- [1]. Attia, H. A. (2010). Unsteady MHD Couette flow of a viscoelastic fluid with heat transfer. *Kragujevac Journal of Science*, 32, pp.5-15.
- [2]. Balvinder Pal Garg, Krishan Dev Singh and A. K. Bansal (2014). Hall current effect on viscoelastic (walter's liquid model-b) MHD oscillatory convective channel flow through a porous medium with heat radiation. *Kragujevac Journal of Science*, 36, pp.19-32.
- [3]. Boussinesq J. (1897). Th'eorie de l'ecoulement tourbillonnant et tumultueux des liquides dans les lits rectilignes a grande section, *Gauthier-Villars Paris 1 Open Library*, OL7070543M.
- [4]. Chamkha, A. (2003). MHD Flow of Uniformly Stretched Vertical Permeable Surface in the Presence of Heat Generation/Absorption and a Chemical Reaction. *International Communications in Heat and Mass Transfer*, 30, pp.413-422. [https://doi.org/10.1016/S0735-1933\(03\)00059-9](https://doi.org/10.1016/S0735-1933(03)00059-9)
- [5]. Dulal Pal and Sukanta Biswas (2018). Magneto hydrodynamic convective-radiative oscillatory flow of a chemically reactive micropolar fluid in a porous medium. *Propulsion and Power Research*, 7(2), pp.158-170
- [6]. Kandasamy, R., Md. Raj, A.W.B. and Khamis, A.B. (2006). Effects of Chemical Reaction, Heat and Mass Transfer on Boundary Layer Flow over a Porous Wedge with Heat Radiation in the Presence of Suction or Injection. *Theoretical Applied Mechanics*, 33, pp.123-148. <https://doi.org/10.2298/TAM0602123K>
- [7]. Khadrawi, A.F. and Al-Odat, M.O. (2005). Transient MHD Free Convection Flow over a Permeable Vertical Moving Plate Embedded in Porous Medium with Uniform Suction. *International Journal of Heat and Technology*, 23, pp.81-87.
- [8]. Kishore, P.M; N.V.R.V.P. Rao, S.V.K.Varma, S.Venkatar-amama (2013). The effects of radiation and chemical reaction on unsteady MHD free convection flow of viscous fluid past an exponentially accelerated vertical. *International Journal of Physical and Mathematical Sciences*, 4 (19), pp.300-317.
- [9]. Mohammad Al Zubi (2018). MHD heat and mass transfer of an oscillatory flow over a vertical permeable plate in a porous medium with chemical reaction. *Modern Mechanical Engineering*, 8, pp.179-191
- [10]. Mebarek-Oudima F. and Makinde O. D. (2018). Numerical simulation of oscillatory MHD natural convection in cylindrical annulus: prandtl number effect. *Defect and Diffusion Forum*, ISSN: 1662-9507, 387, pp. 417-427
- [11]. Pal, D; G.Mandal, (2017). Thermal radiation and MHD effects on boundary layer flow of micropolar manofluid past a stretching sheet with non-uniform heat. *International Journal of Mechanical Science*, 126, pp.308-318.
- [12]. Pradip Kumar Gaur, Abhay Kumar Jha (2016). Heat and mass transfer in visco-elastic fluid through rotating porous channel with hall effect. *Open journal of fluid dynamics*, 6, pp 11-29
- [13]. Reddy, S.K, D.C.Kesavaiah, M.N. RajaShekar, (2013). MHD heat and mass transfer flow of a viscoelastic fluid past an impulsively started infinite vertical plate with chemical reaction. *International Journal of Innovation, Research, Science, Engineering and Technology*, 2 (4), pp. 2319-8753.
- [14]. Sahoo, P. K., Datta, N. and Biswal, S. (2003). Magneto hydrodynamic unsteady free convection flow past an infinite vertical plate with constant suction and heat sink. *Indian Journal of Pure Applied Mathematics*, 34(1), pp. 145 - 155.
- [15]. Sahoo, S. N. (2013). Heat and Mass transfer effect on MHD flow of a viscoelastic fluid through a porous Medium bounded by an oscillating porous plate in Slip flow regime. *International journal of chemical engineering*, Article ID 380679, <http://dx.doi.org/10.1155/2013/380679>

K. K. Asogwa. "Magneto hydrodynamic Oscillatory Viscoelastic Flow with Radiation and Constant Suction over a Vertical Flat Plate in a Porous Medium." *IOSR Journal of Mathematics (IOSR-JM)* 15.6 (2019): 20-30.